Lattice distortion and energy-level structures in doped C_{60} and C_{70} molecules studied with the extended Su-Schrieffer-Heeger model: Polaron excitations and optical absorption

Kikuo Harigaya*
Fundamental Physics Section, Physical Science Division, Electrotechnical Laboratory, Umezono 1-1-4, Tsukuba, Ibaraki 305, Japan
(Received 5 November 1991)

We extend the Su-Schrieffer-Heeger model of polyacetylene to the cases of C_{60} and C_{70} molecules. The results of our numerical calculations of the undoped systems agree well with the known results. When the system (C_{60} or C_{70}) is doped with one or two electrons (or holes), additional charges accumulate nearly along an equatorial line of the molecule. The dimerization becomes weaker along the same line. Two energy levels intrude deeply into the gap; the intrusion is deeper in C_{70} than in C_{60}. Therefore, "polarons" are predicted in doped fullerenes. We calculate the optical-absoprtion coefficient for the C_{60} fullerene in order to consider how the polarons will be observed. It is predicted that an additional absorption peak appears at an energy lower than the intergap transition peaks of the undoped C_{60}. It is found that the C_{60} and C_{70} fullerenes are closely related in their electronic structures as well as lattice geometries.

I. INTRODUCTION

Recently, the fullerenes C_N have been intensively investigated. In particular, the occurrence of the superconductivity in C_{60} crystals doped with alkali metals [$T_c=18$ K for K,[1] $T_c=28$ K for Rb,[2] and $T_c=33$ K for Rb and Cs (Ref. 3)] has attracted much interest in the electronic structure of these undoped and doped systems.

Band-structure calculations[4] of undoped C_{60} crystals have predicted a large energy gap (~ 2 eV), for an insulator. The bands have weak dispersions and their structures reflect molecular orbitals of C_{60}.[5] When C_{60} is doped with alkali-metal atoms, it is expected that the Fermi level is located in weakly dispersive bands. It has been proposed that electrons around the Fermi level condense into a superconducting ground state by attractive interactions, which are mediated particularly by phonons.[6–9] The calculation of C_{70} by the local-density approximation[10] and quantum chemical calculations[11] has also shown the presence of a large energy gap.

Experimental evidence indicates that the electronic structures change when the fullerenes are doped. For example, photoemission studies[12] of C_{60} and C_{70} doped with alkali metals have shown an appearance and shift of peak structures, which cannot be described by a simple band-filling picture. The changes in C_{60} are different from those in C_{70}.

An electron-spin-resonance (ESR) study on the radical anion of C_{60} by Kato *et al.*[13] has revealed a small g factor, $g=1.9991$, and this is associated with the residual orbital angular momentum. It has been suggested that irregular vibrational structure of the electronic absorption may be due to Jahn-Teller distortion. Therefore, it is again confirmed that the lattice and electronic structures of C_{60} change with doping.

In the present paper, we concentrate upon a single C_{60} or C_{70} molecule, and investigate lattice distortion and reconstruction of electronic levels upon doping. It is quite possible that electronic states are spread over the surface of the molecule. Therefore, correlation effects might be neglected in a first approximation. We assume that the effects are renormalized into effective one-electron levels.

First, we describe C_{60} as an electron-phonon system and extend the Su-Schrieffer-Heeger (SSH) model,[14] which was applied successfully for *trans*-polyacetylene. We find that the length difference between the short and long bonds becomes smaller along the equatorial line of the sphere when the changes in the electron number are one and two (the "lightly doped" case). Energy-level structures also change. One energy level splits upward from the fivefold-degenerate highest occupied molecular orbital (HOMO), while the other energy level splits downward from the threefold-degenerate lowest unoccupied molecular orbital (LUMO). The changes are like those in the polaron and bipolaron excitations in polyacetylene and nondegenerate conjugated polymers.[15] The reduction in the degeneracies of wave functions is consistent with that by the Jahn-Teller theorem. Therefore, the symmetry breaking described by the extended SSH model would be one of the realizations of Jahn-Teller distortions. We suggest that these changes might be the origin of the experimental findings on the changes of electronic structures.[12,13] We calculate the optical-absorption coefficient in order to consider how this remarkable change in the energy-level structures can be observed. It is found that an additional absorption peak appears at a much lower frequency than the intergap transition peaks of the undoped C_{60}. Peak positions are mutually different between electron and hole dopings. Our calculations are extended to "heavily doped" systems, too. The electron number is changed between the maximum and minimum numbers, which can be realized in principle. With increasing doping, the average dimerization becomes increasingly weaker. When six electrons are doped, the average is about 0.03 times that of the undoped C_{60}. This value would hardly be observed in experiments. When ten holes are doped, the average is

about 0.5 times. In this case, it is more likely that the dimerization would remain than in the electron-doped case.

Secondly, we investigate possible changes of lattice and electronic systems in the C_{70} molecule, which is present abundantly as is C_{60}. Even though the spatial symmetry of C_{70} is lower than that of C_{60}, we certainly expect that similar, interesting changes might occur as in C_{60}. We show that the extended SSH model well describes the lattice and energy-level structures of the undoped C_{70}, compared with the other results.[10,11] In particular, the same parameters as in C_{60} are valid. Then we calculate for systems where one or two electrons are added or removed. It is predicted that the HOMO and LUMO of the undoped system intrude deeply into the energy gap. The intrusion is deeper in C_{70} than in C_{60}. The lattice pattern deforms from that of the undoped system. We first find that sites, where additional charges favor to accumulate are common to C_{60} and C_{70}. They are along the equatorial line in C_{60}. Wave functions of the intragap levels have large amplitudes at the corresponding sites. This should be considered in the light of the claim that C_{70} is made from C_{60}, by cutting into two parts and adding ten carbon atoms. It is quite interesting that there are relations of electronical properties as well as the structural relation between (doped as well as undoped) C_{60} and C_{70}.

The present paper is a detailed report of two earlier, shorter publications,[16,17] in which partial data have been reported and discussed.

This paper is organized as follows. In Sec. II, the model and the numerical method are explained. In Sec. III, results of C_{60} are shown and discussed. In Sec. IV, we show results of C_{70}. We close the paper with several remarks in Sec. V.

II. MODEL AND NUMERICAL METHOD

The SSH model[14] is extended for the C_{60} and C_{70} molecules:

$$\mathcal{H}=\sum_{\langle ij\rangle,s}[-t_0-\alpha(u_i^{(j)}+u_j^{(i)})](c_{i,s}^{\dagger}c_{j,s}+\text{H.c.}) +\tfrac{1}{2}K\sum_{\langle j\rangle}(u_i^{(j)}+u_j^{(i)})^2 . \tag{2.1}$$

In the first term, the quantity t_0 is the hopping integral of the undimerized systems, α is the electron-phonon coupling; the operator $c_{i,s}$ annihilates a π electron at the ith carbon atom with spin s; $u_i^{(j)}$ is the displacement of the ith atom in the direction of the jth atom (three $u_i^{(j)}$ for the given i are mutually independent); the sum is taken over nearest-neighbor pairs $\langle ij\rangle$. The quantity $u_i^{(j)}+u_j^{(i)}$ is the change of the length of the bond between the ith and jth atoms. When it is possible, the hopping integral increases from t_0; accordingly, we take the sign before α to be negative. The second term is the elastic energy of the phonon system; the quantity K is the spring constant.

The model Eq (2.1) is solved by the adiabatic approximation for phonons. The Schrödinger equation for the π electron is

$$\varepsilon_\kappa\phi_{\kappa,s}(i)=\sum_{\langle ij\rangle}(-t_0-\alpha y_{i,j})\phi_{\kappa,s}(j) , \tag{2.2}$$

where ε_κ is the eigenvalue of the κth eigenstate and $y_{i,j}=u_i^{(j)}+u_j^{(i)}$ is the bond variable. The self-consistency equation for the lattice is

$$y_{i,j}=\frac{2\alpha}{K}\sum_{\kappa,s}{}'\phi_{\kappa,s}(i)\phi_{\kappa,s}(j) -\frac{2\alpha}{K}\frac{1}{N_b}\sum_{\langle kl\rangle}\sum_{\kappa,s}{}'\phi_{\kappa,s}(k)\phi_{\kappa,s}(l) , \tag{2.3}$$

where the prime means the sum over the occupied states, the last term is due to the constraint $\sum_{\langle ij\rangle}y_{i,j}=0$, and N_b is the number of π bonds. We use $N_b=90$ for C_{60} and $N_b=105$ for C_{70}. The same constraint has been used in polyacetylene[18] in order to numerically obtain a correct dimerized ground state of the undoped system. We can certainly assume that the constraint works well for the present systems, too. Owing to the constraint, we can avoid the contraction of the lattice; the total energy width from the lowest occupied molecular orbital to the highest unoccupied molecular orbital does not vary from that of the undimerized system. A numerical solution is obtained in the following way:

(i) Random numbers between $-y_0$ and y_0 ($y_0=0.1$ Å) are generated for the initial values of the bond variables $\{y_{i,j}^{(0)}\}$. Then we start the iteration.

(ii) At the kth step of the iteration, the electronic part of the Hamiltonian is diagonalized by solving Eq. (2.2) for the set of the bond variables $\{y_{i,j}^{(k)}\}$.

(iii) Using the electronic wave functions $\{\phi_{\kappa,s}(i)\}$ obtained above, we calculate the next set $\{y_{i,j}^{(k+1)}\}$ from the left-hand side of Eq. (2.3).

(iv) The iteration is repeated until the sum $\sum_{\langle i,j\rangle}[y_{i,j}^{(k+1)}-y_{i,j}^{(k)}]^2$ becomes negligibly small.

(v) It is checked that there is only one stationary solution for each electron number by changing the initial random set $\{y_{i,j}^{(0)}\}$ and the maximum value y_0. Here we consider that possible degenerate solutions with respect to the geometrical direction of these fullerene molecules are an identical solution.

III. UNDOPED AND DOPED C_{60} MOLECULES

We take $t_0=2.5$ eV, because a tight-binding model with the same value well reproduces the band structure of a two-dimensional graphite plane.[19] The same value is used in polyacetylene.[14] This indicates that the origin of t_0 is common. It is quite interesting to point out that the same parameter t_0 is valid for three different systems: graphite, polyacetylene, and C_N. Therefore, the overlap of π orbitals of nearest-neighbor carbon atoms is almost independent of kinds of material, even though bond lengths and bonding angles are different.

Two quantities, α and K, are determined so that the length difference between the short and long bonds is the experimentally observed value: 0.05 Å.[20] Here, the dimensionless electron-phonon coupling $\lambda\equiv 2\alpha^2/\pi K t_0$ is taken as 0.2 as in polyacetylene.[14] The choice of λ stands upon the analogy that the general parameters of π-conjugated carbon systems do not vary so widely. The result is $\alpha=6.31$ eV/Å and $K=49.7$ eV/Å^2. This choice

of the parameters are valid enough, in view of the fact that the resulting energy gap of the undoped system (2.255 eV) agrees with about 1.9 eV of the other result[5] within 20%. The sensitivity of the choice of parameters does not depend on the qualitative results of this paper; for example, intrusion of levels, lattice distortion patterns, and so on.

The number of electrons N_{el} is varied within $N-10 \le N_{el} \le N+6$, where $N(=60)$ is the number of carbon atoms. When $N_c \equiv N_{el}-N$ is positive, the system is doped with electrons. If $N_c<0$, the system is doped with holes. In principle, the maximum additional electron and hole numbers are 6 and 10, respectively. We calculate for all possible N_c. For convenience, we call the systems with $|N_c|=1,2$ lightly doped C_{60}. We denote the systems with $|N_c| \ge 3$ as heavily doped C_{60}. We report the lightly doped cases separately, because quite interesting changes are found for these cases.

A. Undoped and lightly doped C_{60}

First we show lattice and electronic structures. Magnitudes of the bond variable are presented in Table I for $-2 \le N_c \le 2$. Configurations of the lattice are shown in Fig. 1. The excess electron densities at each site are listed in Table II. This quantity is calculated by $[\sum'_{\kappa,s} \phi^2_{\kappa,s}(i)]-1$. When the system is undoped, there are 30 short bonds and 60 long bonds. They are shown in Fig. 1(a). All the sides of the pentagons are the single bonds. The double and single bonds alternate along the sides of the hexagons. This feature is in agreement with that in the previous study.[5,19] The lattice configurations of the doped systems are shown in Figs. 1(b) and 1(c). The symbols labeling the bonds, from *a* to *g*, indicate the corresponding bond variables in Table I. We show three kinds of shorter bond. The shortest bonds, namely *d*, are represented by making use of the thick lines. The second shortest ones, *b*, are shown by the usual double lines. The dashed lines indicate the third shortest bonds. They are the bonds *f* in Fig. 1(b) and bonds *g* in Fig. 1(c). Other longer bonds are not shown for simplicity. The symbols labeling the sites, from *A* to *D*, show relations with the electron density in Table II. The figures are the same for the electron and hole dopings. When the change in the number of electrons is one, the change in the electron density is the largest at the sites at the ends of dashed lines, namely points *D*. The dashed lines are located

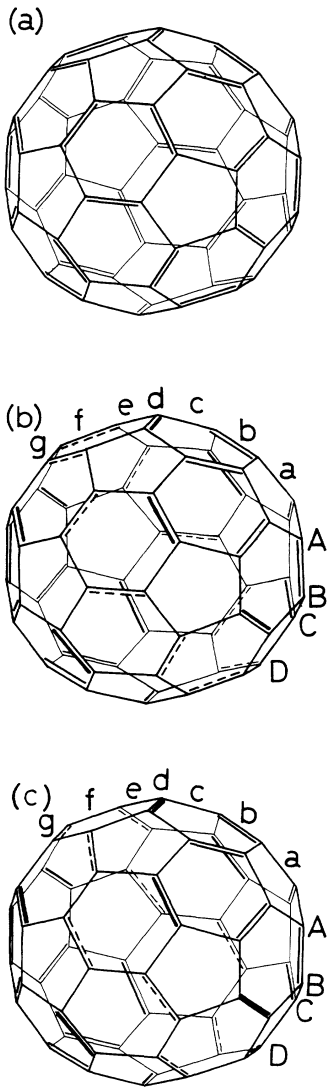

FIG. 1. Lattice configurations of (a) the undoped C_{60}, (b) the doped C_{60} with $|N_c|=1$, and (c) the doped C_{60} with $|N_c|=2$. The figures are common to electron and hole dopings. The symbols indicate names of bonds and lattice sites. In (a), short bonds are shown by the double lines. In (b) and (c), three kinds of the shorter bonds are shown. The thick lines indicate the shortest bonds, while the dashed lines are for the third shortest bonds.

TABLE I. The bond variable for the undoped and doped C_{60} with $-2 \le N_c \le 2$. The bond length becomes longer from the top to the bottom. Valves are in Å. We show the symbols that indicate the positions in Fig. 1 and the number of bonds of the same length in the square brackets.

$N_c=0$	1	2	−1	−2
0.033 33[30]	0.032 73[*d*,10]	0.03236[*d*,10]	0.038 08[*d*,10]	0.043 16[*d*,10]
−0.016 67[60]	0.029 45[*b*,10]	0.025 78[*b*,10]	0.034 47[*b*,10]	0.035 65[*b*,10]
	0.020 32[*f*,10]	0.010 56[*g*,10]	0.020 99[*f*,10]	0.014 28[*g*,10]
	−0.003 28[*g*,10]	0.006 96[*f*,10]	−0.001 23[*g*,10]	0.009 61[*f*,10]
	−0.014 42[*a*,10]	−0.012 22[*a*,10]	−0.015 95[*a*,10]	−0.015 19[*a*,10]
	−0.014 97[*c*,20]	−0.012 99[*c*,20]	−0.015 96[*c*,20]	−0.015 20[*c*,20]
	−0.017 42[*e*,20]	−0.018 73[*e*,20]	−0.022 21[*e*,20]	−0.028 05[*e*,20]

TABLE II. The excess electron density per site of doped C_{60}. The symbols indicate the positions of lattice sites shown in Fig. 1.

Position	$N_c=1$	2	−1	−2
A	0.004 75	0.009 23	−0.001 08	−0.002 14
B	0.022 26	0.042 49	−0.000 59	−0.001 22
C	0.001 45	0.003 34	−0.011 00	−0.022 67
D	0.035 04	0.070 80	−0.038 17	−0.075 65

nearly along an equatorial line of C_{60}. The absolute value of the length of the bonds *g* is the smallest of the four kinds of bond with negative bond variables. This implies that the dimerization is weakest along this equatorial line. The change in the density is the smallest at the sites at the ends of the thick lines, points *C*, when the electron is doped. It is the smallest at points *B*, when the hole is doped. The order of points *B* and *C* with respect to the excess electron density is interchanged. This is one of the consequences of the lack of the electron-hole symmetry. A remarkable feature, i.e., the distortion of the lattice, is similar to that of a polaron[15] in polyacetylene; the spatial phase of the alternation of short and long bonds does not change upon doping, and the lattice distortion is the largest (the dimerization is the weakest) where the change in the local electron density is the largest. Therefore, we conclude that the lightly doped system has lattice structures and electron distributions like those in a polaron of polyacetylene. When the change in the electron number is two, configurations of dashed lines along the equatorial line change, as shown in Fig. 1(c). The ordering of bonds *f* and *g* with respect to the bond variable is reversed. Other configurations are the same. The change in the electron density is the largest at points *D*, too. Therefore, polaronic distortion persists when the doping proceeds from one to two electrons (or holes). This can be compared with a bipolaron formation in nondegenerate conjugated polymers.[15] However, this distortion is polaron-like.

Next we look at changes in the electronic level structures. Figure 2(a) shows results of the undoped and electron-doped systems, while Fig. 2(b) is for the hole-doped systems. The line length is proportional to the degeneracy of a level. The shortest line is for the nondegenerate level. The arrow indicates the position of the Fermi level. It is located between energy levels when N_{el} is even. It is located just at one level if N_{el} is odd; the energy level at the Fermi level is singly occupied. In the undoped system, the HOMO is fivefold degenerate. The LUMO is threefold degenerate. This is a consequence of the lattice geometry.[5] Similarly, energy differences between energy levels remarkably reproduce other results.[5,19] Therefore, the extended SSH model well describes the electronic structures of undoped C_{60}. This is due to the fact that eigenstates around the gap originate mainly from π electrons. We note that here the electron-hole symmetry of the SSH model for polyacetylene is lacking. This is a consequence of the fact that three bonds are connected to each carbon atom. Thus, the present system is rather similar to nondegenerate conjugated polymers.

When the system is doped, the degeneracy decreases due to the reduced symmetry. This reduction comes from the deformation of the lattice. This feature of the removal of the degeneracy coincides with that of the Jahn-Teller theorem. Therefore, the lattice deformation would be one of the possible realizations of Jahn-Teller distortions. In Ref. 8, it is predicted that phonon modes with H_g symmetry might couple largely with electrons in doped C_{60}. This H_g Jahn-Teller coupling has the same symmetry as in the present work: the static distortions of the lightly doped systems are driven by phonons with H_g symmetry. The removal of degeneracies of energy levels has the same splitting patterns due to the H_g distortion, as shown in Fig. 2 of Ref. 8. When $|N_c|=1$ and 2, the highest level, which splits from the HOMO of the undoped system, is nondegenerate. Its energy shifts upward. In contrast, the other two levels shift only slightly.

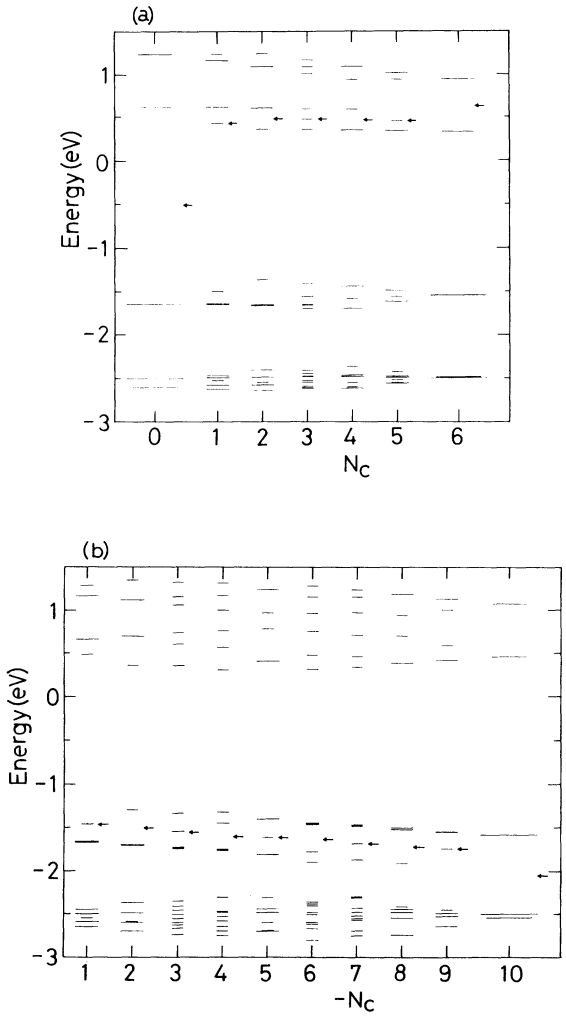

FIG. 2. Energy-level structures of (a) the undoped and electron-doped C_{60}, and (b) hole-doped C_{60}. The line length is proportional to the degeneracy of the energy level. The shortest line is for the undegenerate levels. The arrow indicates the position of the Fermi level.

Similarly, the LUMO of the undoped system splits into two levels. The energy of the nondegenerate level shifts downward, while the change of the energy of the doubly degenerate level is small. This change in the level structures is common to two cases of the electron and hole dopings. The change is similar to that in the polaron formation[15] in polyacetylene; two nondegenerate levels split into the gap from the valence and conduction bands, without a change in the gap width. This feature coincides with the consequences by the lattice and electron distributions described above. Since effects of various terms, such as the correlation among electrons, Coulomb potentials due to charged dopant ions, and possible hopping interactions between C_{60} molecules, are expected to be small, it is quite possible that the above change of electronic structures can be observed in experiment, for example, in optical absorption.

B. Heavily doped C_{60}

When the doping proceeds further for larger $|N_c|$, the level structures change complexly. When electrons are doped, all the degeneracies are removed at $N_c=3$. Some degeneracies revive at $N_c=4$ and 5, and the structure of degeneracies at $N_c=6$ is like that of the undoped system. When holes are doped, all the levels are undegenerate at $-N_c=3$, 4, 6, and 7. There are singly and doubly degenerate levels at $-N_c=5$, 8, and 9. Again, the structure of the degeneracies at $-N_c=10$ is like that of the undoped system. In Fig. 2, the structures of the degeneracies show that there is an apparent symmetry between $N_c=1$ and 5, $N_c=2$ and 4, $-N_c=1$ and 9, etc. We note that those symmetries should be due to the Jahn-Teller-type energy gain.

The lattice structures are very complex for $|N_c|\geq 3$. For example, when $N_c=3$, there are 45 kinds of bond length and only two of all the bands have the same length. The symmetry of the doped C_{60} molecule is reduced strongly. Because it is difficult to illustrate these lattice patterns, it would be more helpful if we discuss instead global features of the changes in these lattice patterns. Therefore, we calculate the mean absolute values $\langle |y_{i,j}| \rangle$ of the bond variable. Table III shows the results. As $|N_c|$ increases, the average dimerization becomes weaker and weaker. When six electrons are doped, the average is about 0.03 times that of the undoped C_{60}. The dimerization can hardly be observed in experiment. In particular, lattice fluctuations from the classical displacements may smear out the very small dimerization even in low temperatures. When ten holes are doped, the average becomes about 0.5 times. In this case, the possibility that the dimerization would remain and be observed is larger than that in the electron-doped case. In Ref. 6, the dimerization strength of the electron-doped systems is calculated with the assumption that all of the short bonds change their lengths by the same value and all of the long bonds do so as well. In the present paper, all of the bond variables are chosen independently. However, the dimerization is of a magnitude similar to that in Ref. 6.

We calculate the total energy gain from that of the undoped system, and present the results in Table III. When electrons are doped, the energy gain increases with the electron number. This indicates that electrons are easily absorbed by the molecule. In fact, the maximum number $N_c=6$ has been obtained experimentally.[12] When holes are doped, the energy gain saturates at $-N_c=4$. It has the maximum at $-N_c=6$, and becomes rather small at $-N_c=9$ and 10. This saturation and reduction of the gain would be related with the more strongly persisting dimerization in the hole-doped systems than in the electron-doped ones. This behavior reflects the lack of electron-hole symmetry in C_{60}.

TABLE III. The mean absolute values of the bond variable $\langle |y_{i,j}| \rangle$ for the undoped and doped C_{60} with $-10\leq N_c\leq 6$. The total energy gain from that of the undoped system is also shown.

N_c	$\langle |y_{i,j}| \rangle$ (Å)	Energy gain (eV)
0	0.022 22	
1	0.018 33	0.0626
2	0.016 81	0.2542
3	0.012 42	0.3333
4	0.010 35	0.5386
5	0.005 06	0.6331
6	0.000 61	0.8516
−1	0.020 79	0.0852
−2	0.022 60	0.3420
−3	0.020 79	0.3567
−4	0.021 03	0.5180
−5	0.018 83	0.4894
−6	0.017 11	0.5713
−7	0.014 91	0.4715
−8	0.013 81	0.5123
−9	0.010 82	0.3211
−10	0.009 73	0.2930

C. Optical absorption

We shall discuss how the "polarons" can be observed in experiment. In particular, we calculate the optical-absorption coefficient (dynamical conductivity). Our calculations are strongly related to low-energy experiments of radical anions and cations. Furthermore, optical absorption of doped lattice systems is interesting, because the hopping integral between C_{60} molecules is very small and is negligible in a first approximation, as recent band-structure calculations[4] indicate.

The present calculation is performed with the help of the standard Kubo formula and information on coordinates of lattice points of the truncated icosahedron. The small lattice displacements are not considered when the system is doped. This is a valid approximation because the deformations in the geometries of dipole moments are a higher-order effect, in view of the treatment by the simple extended SSH model, where we neglect a possible coupling of electrons with phonon modes due to bond-angle modulations and effects of off-planar geometry around carbon atoms.

Figure 3 shows the results of undoped and electron-

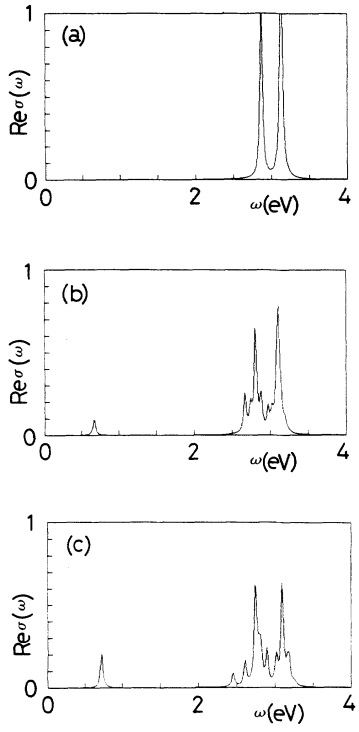

FIG. 3. Optical absorption of the undoped and electron-doped C_{60}. The unit of the ordinate is arbitrary. In (a), the result of the undoped C_{60} is shown. (b) and (c) are the data of the systems with $N_c=1$ and 2, respectively.

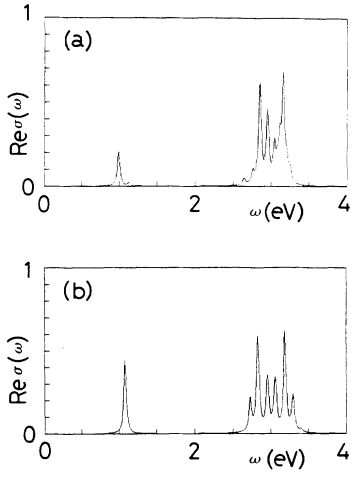

FIG. 4. Optical absorption of the hole-doped C_{60}. The unit of the ordinate is arbitrary. (a) and (b) are the data of the systems with $-N_c=1$ and 2, respectively.

doped systems with $0\le N_c\le 2$, while Fig. 4 is for the hole-doped systems with $-N_c=1$ and 2. We only show data of the lightly doped cases, because the general features found in changes of the absorption patterns persist with higher doping. We adopt a Gaussian broadening procedure with the width 0.02 eV. Figure 3(a) is the data of the undoped system. There are two peaks in the figure. The peak at 2.9 eV is the transition between the HOMO and the next lowest unoccupied molecular orbital. The other peak at 3.1 eV is the transition between the next highest occupied molecular orbital and the LUMO. The two transitions are allowed ones. The transition between the HOMO and the LUMO is forbidden and does not appear in the figure. These well-known features[4,5] are reproduced in the present calculation. Figures 3(b) and 3(c) show the data of the systems with $N_c=1$ and 2, respectively. The two large peaks in Fig. 3(a) now have small substructures due to the level splittings. An additional peak appears at a lower energy ($\sim$0.7 eV). This peak corresponds to the transition between the singly occupied molecular orbital and the next lowest unoccupied molecular orbital, etc., when $N_c=1$. It corresponds to the transition between the LUMO and the next lowest unoccupied molecular orbital, etc., when $N_c=2$. Therefore, this peak at low energy is a consequence due mainly to the splitting of the LUMO of the undoped system. Similar changes are found for hole-doped systems. Figures 4(a) and 4(b) show the data for $-N_c=1$ and 2, respectively. The two main peaks in Fig. 3(a) become broad and have small structures upon doping. There appears also an additional peak. The energy at about 1 eV is different from that of the electron-doped systems. This is due to the lack of the electron-hole symmetry. This peak is again the consequence of the splitting of energy levels by the doping.

IV. UNDOPED AND DOPED C_{70} MOLECULES

We take the same parameters as in C_{60}, because effects due to the difference in geometrical structures are expected to be small. The number of electrons, N_{el}, is varied within $N-2\le N_{el}\le N+2$ ($N=70$), because the lightly doped cases are particularly interesting.

Figure 5 shows the geometrical structures in real space. Symbols $a-h$ label the bonds. Symbols $A-E$ label the lattice points. In Table IV, we present the values of the bond variable $y_{i,j}$. In Fig. 5, we show only four kinds of shorter bond for simplicity. The double lines with a heavy line indicate the shortest bonds. The normal double lines are for the second shortest bonds. The double lines with dashed and dash-dotted lines depict the third and fourth shortest bonds, respectively.

First we discuss results of the undoped C_{70}. Figure 5(a) shows the lattice pattern. The length difference between the shortest and longest bonds is about 0.057 Å, which agrees well with the value 0.06 Å used in Ref. 10. We also find that the energy difference between the HOMO and the LUMO, 1.65 eV, agrees with that in Ref. 10. Therefore, it is shown that the same parameters used for C_{60} are realistic for C_{70}. This means that parameters of the extended SSH model do not sensitively depend on whether the shape of the molecule resembles spheroid or ellipsoid. However, there is a structural difference from Ref. 10. The length difference between the bonds, f and g, is about 0.001 Å and very small. The dimerization almost disappears at hexagons constructed by bonds f and g. These hexagons are similar to benzene rings. This

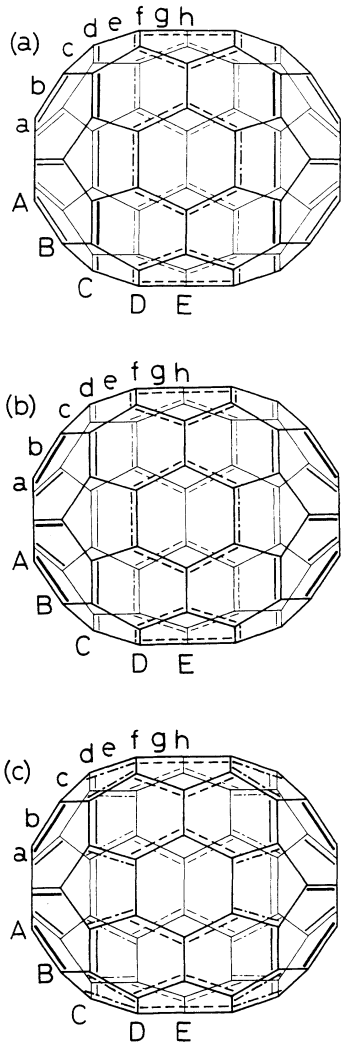

FIG. 5. Lattice configurations for (a) the undoped C_{70}, (b) the doped C_{70} with $|N_c|=1$, and (c) the doped C_{70} with $|N_c|=2$. The figures are common to electron and hole hopings. The symbols are names of bonds and lattice sites. The double lines with a heavy line indicate the shortest bonds. The normal double lines are for the second shortest bonds. The double lines with dashed and dash-dotted lines depict the third and fourth shortest lines, respectively.

property coincides with that of the quantum chemical calculations in Ref. 11. In Fig. 5(a), the alternation of short and long bonds is present in the left and right parts of the figure, along bonds from $a-e$. It is often claimed that C_{70} can be made by cutting C_{60} into two parts and adding ten more carbon atoms between them. The positions of the dimerization, which remains in C_{70}, correspond to those in C_{60}. Table V shows the electron density. The electron distribution is not uniform, different from the undoped C_{60}. Spatial oscillation, from site A to E, is seen. This might be caused by the distorted structure of C_{70}.

Next we look at changes in lattice structures and electron distributions of the doped C_{70}. Figure 5(b) shows the lattice configuration when one electron is added or removed. Figure 5(c) depicts the case where two electrons are added or removed. Figures are common to electron and hole dopings. When one electron is added to or removed from the undoped C_{70}, the two kinds of bonds with heavy and normal lines are interchanged. Positions of the other bonds shown by dashed and dash-dotted lines do not change. When one electron is added or removed further, bonds with dash-dotted lines change their positions. Other shorter bonds do not interchange. Through this development, the patterns with the mirror reflection symmetry are retained. This is the consequence of the more elongated shape. In Table VI, we list the excess electron density, where the electron density of the undoped system is subtracted. The change in electron density at sites E is very small. This is the consequence of the fact that dimerization almost disappears along bonds f and g in the undoped C_{60}. The part along the equatorial line has a property similar to that of the graphite plane. The strengths of the dimerization change largely along bonds $a-e$ upon doping. The additional charges favor accumulation near these bonds. Therefore, the density of the additional charge would be very small at site E. The positions D, where the additional charges accumulate most densely, correspond to the sites D of C_{60} in Fig. 1. These sites lie along the equatorial line of C_{60}. When we make C_{70} from C_{60}, sites E are added in the interval. But the property that additional charges favor to accumulate at sites D persists for C_{70}. We believe that this finding is quite interesting.

Finally, we show structures of electronic energy levels

TABLE IV. The bond variable for undoped and doped C_{70}. The bond length becomes longer from the top to the bottom. Values are in Å. We show the symbols that indicate the positions in Fig. 5 and the number of bonds of the same length in the square brackets.

$N_c=0$	1	2	−1	−2
0.035 14[d,10]	0.031 26[b,10]	0.031 46[b,10]	0.037 21[b,10]	0.043 46[b,10]
0.031 14[b,10]	0.024 81[d,10]	0.014 19[d,10]	0.032 00[d,10]	0.028 76[d,10]
0.010 09[g,20]	0.010 10[g,20]	0.009 06[g,20]	0.011 22[g,20]	0.011 33[g,20]
0.010 30[g,10]	−0.000 75[f,10]	0.001 50[e,20]	−0.000 31[f,10]	−0.004 87[e,20]
−0.015 32[c,20]	−0.010 47[e,20]	−0.011 04[h,5]	−0.013 21[h,5]	−0.010 89[f,10]
−0.015 35[h,5]	−0.013 29[h,5]	−0.012 12[f,10]	−0.013 56[e,20]	−0.010 94[h,5]
−0.016 06[a,10]	−0.015 71[c,20]	−0.016 11[c,20]	−0.019 11[c,20]	−0.022 84[a,10]
−0.022 20[e,20]	−0.016 51[a,10]	−0.016 81[a,10]	−0.019 40[a,10]	−0.022 97[c,20]

TABLE V. The electron density per site of the undoped C_{70}. The symbols indicate positions of lattice sites shown in Fig. 5.

Position	$N_c=10$
A	0.991 99
B	1.012 46
C	0.995 40
D	1.011 51
E	0.981 74

in Fig. 6. As in C_{60}, electronic states around the LUMO and HOMO are originated mainly from π electrons. Therefore, results are reliable as far as we look at levels only around the Fermi level. This energy region is particularly interesting in optical-absorption experiments. In Fig. 6, energy levels in the region from -3 to 5 eV are shown varying the electron number. The notations are the same as those in Fig. 2. When the system is half-filled, the HOMO and LUMO are nondegenerate. The energy difference between them is 1.65 eV, which is comparable to that of C_{60} (2.26 eV). Positions and degeneracies of other levels below the HOMO and above the LUMO show an overall agreement with the other result.[10] This clearly indicates the validity of the extended SSH model. The energy difference between the HOMO and the next highest occupied level is much smaller than the width of the gap. Similarly, the energy difference between the LUMO and the next lowest unoccupied level is small. This is a consequence of the smallness of the structural perturbation from C_{60} to C_{70}. The structure of the degeneracies (the property that there are onefold- and twofold-degenerate levels) is like that in C_{60} where one or two electrons (or holes) are doped. This is due to the same symmetry of those systems. When the system is doped with up to two electrons or holes, a significant change is predicted. The HOMO and LUMO of the undoped system apparently extend into the gap. The positions of the other levels change only slightly. This property has also been found in doped C_{60}. We have named this change the "polaronlike change" in polyacetylene. The magnitude of the level intrusion is larger in C_{70} than that in C_{60}. This is a consequence of the fact that levels near the gap have already split at $N_c=0$. The HOMO and LUMO of the undoped system have large amplitude at sites $A-D$. The amplitude at D is the largest. The amplitude at E is very small. Therefore, the additional charges favor accumulation at sites D.

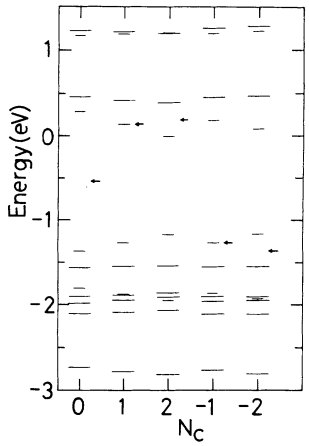

FIG. 6. Energy-level structures around the HOMO and LUMO of the undoped and doped C_{70}. The line length is proportional to the degeneracy of the energy level. The shortest line is for the undegenerate levels. The arrow indicates the position of the Fermi level.

V. CONCLUDING REMARKS

We have applied the extended SSH model to undoped and doped C_{60} and C_{70}. The calculations of the undoped system (C_{60} or C_{70}) agree well with the known results.[5,10,11] When the system is doped with one or two electrons (or holes), the additional charges accumulate nearly along an equatorial line of the molecule. The dimerization becomes weaker nearly along the same line. In the energy-level structure, two levels intrude deeply into the gap. These changes are characteristic of "polaron excitatons" on conjugated polymers.[15] We have discussed that the changes can be observed experimentally, for example, in optical-absorption measurements, and have calculated the dynamical conductivity for C_{60} in order to look at how they can be observed. It is predicted that there an additional peak appears at an energy lower than the intergap transition peaks.

We have found that sites where additional charges prefer to accumulate are common to C_{60} and C_{70}. They are along the equatorial line in C_{60}. In C_{70}, ten more atoms are inserted among these sites. Wave functions of the intragap levels have large amplitudes at corresponding sites, too. The additional charges occupy these wave functions, and thus the sites where the additional charge density is larger are common. This should be considered

TABLE VI. The excess electron density per site of the doped C_{70}. The symbols indicate positions of lattice sites in Fig. 5.

Position	$N_c=1$	2	-1	-2
A	$-0.003\,62$	$-0.007\,05$	$-0.012\,56$	$-0.025\,04$
B	0.002 15	0.004 42	$-0.013\,18$	$-0.027\,08$
C	0.024 99	0.044 97	$-0.007\,14$	$-0.014\,43$
D	0.026 10	0.052 03	$-0.030\,16$	$-0.059\,89$
E	$-0.000\,72$	$-0.001\,38$	0.000 34	0.000 75

in view of the claim that C_{70} is made from C_{60} by cutting into two parts and adding ten more carbon atoms. It is quite interesting that there are relations with respect to electronical properties as well as the above-mentioned structural relation between (doped as well as undoped) C_{60} and C_{70}.

We have not considered various other effects, because the present study is at a first stage of the investigation. Electron correlations among electrons might have an effect on energy-level structures, particularly when the Fermi level lies just at one energy level. Fluctuation of phonons from the classical mean field might affect the stability of the polaronic distortions. Interactions between molecules could be problematical, also: it is an important problem to clarify how our findings will persist, especially in the case of doped crystals. These neglected contributions pose interesting problems for future investigations.

Recently, after the submission of a previous paper,[16] we found that Friedman[21] has independently performed a similar calculation of electron-doped C_{60}. Our results agree where comparisons are possible.

ACKNOWLEDGMENTS

Fruitful discussions with Dr. K. Yamaji, Dr. S. Abe, Dr. Y. Asai (Electrotechnical Laboratory), Dr. A. Terai (University of Tokyo), Dr. N. Hamada, Dr. S. Saito, and Dr. A. Oshiyama (Fundamental Research Laboratories, NEC Corporation) are acknowledged. The author thanks Professor B. Friedman (Sam Houston State University) for sending a report of his work prior to publication.

*Electronic mail address: e9118@etlcom1.etl.go.jp, e9118@jpnaist.bitnet.

[1]A. F. Hebard, M. J. Rosseinsky, R. C. Haddon, D. W. Murphy, S. H. Glarum, T. T. M. Palstra, A. P. Ramirez, and A. R. Kortan, Nature **350**, 600 (1991).

[2]M. J. Rosseinsky, A. P. Ramirez, S. H. Glarum, D. W. Murphy, R. C. Haddon, A. F. Hebard, T. T. M. Palstra, A. R. Kortan, S. M. Zahurak, and A. V. Makhija, Phys. Rev. Lett. **66**, 2830 (1991).

[3]K. Tanigaki, T. W. Ebbesen, S. Saito, J. Mizuki, J. S. Tsai, Y. Kubo, and S. Kuroshima, Nature **352**, 222 (1991).

[4]S. Saito and A. Oshiyama, Phys. Rev. Lett. **66**, 2637 (1991).

[5]M. Ozaki and A. Takahashi, Chem. Phys. Lett. **127**, 242 (1986); S. Saito, in *Clusters and Cluster Assembled Materials,* edited by R. S. Averback, D. L. Nelson, and J. Bernholc (Materials Reserach Society, Pittsburgh, 1991).

[6]F. C. Zhang, M. Ogata, and T. M. Rice, Phys. Rev. Lett. **67**, 3452 (1991).

[7]Y. Asai (unpublished).

[8]C. M. Varma, J. Zaanen, and K. Raghavachari, Science **254**, 989 (1991).

[9]M. J. Rice, H. Y. Choi, and Y. R. Wang, Phys. Rev. B **44**, 10414 (1991).

[10]S. Saito and A. Oshiyama, Phys. Rev. B **44**, 11 532 (1991).

[11]G. E. Scuseria, Chem. Phys. Lett. **180**, 451 (1991); J. Baker, P. W. Fowler, P. Lazzeretti, M. Malagoli, and R. Zanasi, *ibid.* **184**, 182 (1991).

[12]T. Takahashi, T. Morikawa, S. Sato, H. Katayama-Yoshida, A. Yuyama, K. Seki, H. Fujimoto, S. Hino, S. Hasegawa, K. Kamiya, H. Inokuchi, K. Kikuchi, S. Suzuki, K. Ikemoto, and Y. Achiba, Physica C **185-189**, 417 (1991); C. T. Chen, L. H. Tjeng, P. Rudolf, G. Meigs, L. E. Rowe, J. Chen, J. P. McCauley, Jr., A. B. Smith III, A. R. McGhie, W. J. Romanow, and E. W. Plummer, Nature **352**, 603 (1991).

[13]T. Kato, T. Kodama, M. Oyama, S. Okazaki, T. Shida, T. Nakagawa, Y. Matsui, S. Suzuki, H. Shiromaru, K. Yamauchi, and Y. Achiba, Chem. Phys. Lett. **180**, 446 (1991).

[14]W.-P. Su, J. R. Schrieffer, and A. J. Heeger, Phys. Rev. B **22**, 2099 (1980).

[15]A. J. Heeger, S. Kivelson, J. R. Schrieffer, and W.-P. Su, Rev. Mod. Phys. **60**, 781 (1988).

[16]K. Harigaya, J. Phys. Soc. Jpn. **60**, 4001 (1991).

[17]K. Harigaya, Chem. Phys. Lett. **189**, 79 (1992).

[18]K. Harigaya, A. Terai, Y. Wada, and K. Fesser, Phys. Rev. B **43**, 4141 (1991).

[19]G. W. Hayden and E. J. Mele, Phys. Rev. B **36**, 5010 (1987).

[20]C. S. Yannoni, P. P. Bernier, D. S. Bethune, G. Meijer, and J. R. Salem, J. Am. Chem. Soc. **113**, 3190 (1991).

[21]B. Friedman, Phys. Rev. B **54**, 1454 (1992).